Author/s:
Leiske, MN;Lai, M;Amarasena, T;Davis, TP;Thurecht, KJ;Kent, SJ;Kempe, K

Title:
Interactions of core cross-linked poly(2-oxazoline) and poly(2-oxazine) micelles with immune cells in human blood

Date:
2021-07

Citation:
Leiske, M. N., Lai, M., Amarasena, T., Davis, T. P., Thurecht, K. J., Kent, S. J. & Kempe, K. (2021). Interactions of core cross-linked poly(2-oxazoline) and poly(2-oxazine) micelles with immune cells in human blood. Biomaterials, 274, https://doi.org/10.1016/j.biomaterials.2021.120843.

Interactions of core cross-linked poly(2-oxazoline) and poly(2-oxazine) micelles with immune cells in human blood

Meike N. Leiske,[a] May Lai,[a] Thakshila Amarasena,[b,c] Thomas P. Davis,[a,d] Kristofer J. Thurecht,[d] Stephen J. Kent,[b,c,e]* Kristian Kempe[a,f,]*

[a]ARC Centre of Excellence in Convergent Bio-Nano Science & Technology, and Drug Delivery, Disposition and Dynamics, Monash Institute of Pharmaceutical Sciences, Monash University, Parkville, VIC 3052, Australia

[b]ARC Centre of Excellence in Convergent Bio-Nano Science and Technology, The University of Melbourne, Melbourne, Australia

[c]Department of Microbiology and Immunology, Peter Doherty Institute for Infection and Immunity, The University of Melbourne, Melbourne, Victoria 3000, Australia

[d]Centre for Advanced Imaging (CAI) and Australian Institute for Bioengineering and Nanotechnology, ARC Centre of Excellence in Convergent Bio-Nano Science and Technology and ARC Training Centre for Innovation in Biomedical Imaging Technology, The University of Queensland, St. Lucia, QLD 4072, Australia

[e]Melbourne Sexual Health Centre and Department of Infectious Diseases, Alfred Health, Central Clinical School, Monash University, Melbourne, Victoria 3800, Australia

[f]Materials Science and Engineering, Monash University, Clayton, VIC 3800, Australia

Abstract

Water-soluble poly(cyclic imino ether)s (PCIEs) have emerged as promising biocompatible polymers for nanomedicine applications in recent years. Despite their generally accepted stealth properties, there has been no comprehensive evaluation of their interactions with primary immune cells in human blood. Here we present a library of core cross-linked micelles (CCMs) containing various PCIE shells. Well-defined high molar mass CCMs (M_n > 175 kDa, Đ < 1.2) of similar diameter (~20 nm) were synthesised using a cationic ring-opening polymerisation (CROP) – surfactant-free reversible addition-fragmentation chain-transfer (RAFT) emulsion polymerisation strategy. The stealth properties of the different PCIE CCMs were assessed employing a whole human blood assay simulating the complex blood environment. Cell association studies revealed lower associations of poly(2-methyl-2-oxazoline) (PMeOx) and poly(2-ethyl-2-oxazoline) (PEtOx) CCMs with blood immune cells compared to the respective poly(2-oxazine) (POz) CCMs. Noteworthy, PMeOx CCMs outperformed all other reported CCMs, showing overall low associations and only negligible differences in the presence and absence of serum proteins. This study highlights the importance of investigating individual nanomaterials under physiologically-

relevant conditions and further strengthens the position of PMeOx as a highly promising stealth material for biomedical applications.

Keywords

Cyclic imino ether, emulsion polymerisation, immune cell interaction, core cross-linked micelle, stealth effect, RAFT polymerisation

Introduction

The fabrication or surface modification of nanoparticles with water-soluble and biocompatible stealth materials is considered one of the critical design criteria for nanomedicines which require long blood circulation times and limited nonspecific interactions with biomolecules.[1, 2] Similarly, drugs are reversibly modified with stealth polymers to increase their solubility, biocompatibility, and blood circulation times.[3-5] To date, the only polymer approved by the U. S. Food and Drug Administration (FDA) exhibiting these characteristics is poly(ethylene glycol) (PEG), *e.g.* as PEGylated protein pharmaceuticals and for the conjugation of small molecules.[6, 7] Despite the beneficial properties of PEG, concerns about the future potential of PEGylated therapeutics have been raised due to the generation of anti-PEG antibodies, even in individuals who have not been exposed to PEG-based therapeutics previously.[8] Moreover, changes in their pharmacokinetic behaviour after repeated injections (accelerated blood clearance phenomenon),[9] stress related degradation as well as the formation of toxic by-products such as 1,4-dioxane during the synthesis process have been observed.[6, 7, 10] It is apparent that alternative polymeric stealth materials for biomedical applications are needed to address the challenges of this field in the future.

Apart from poly(*N*-(2-hydroxypropyl)methacrylamide), poly(zwitterion)s, poly(peptide)s, and other low fouling systems,[10-12] polymers made from cyclic imino ethers (CIEs) represent powerful alternatives to PEG. Since their development in the 1960s,[13-16] interest in the polymer class of poly(2-oxazoline)s (POx) has grown significantly. Extensive fundamental studies have generated in-depth knowledge about the polymerisation behaviour of differently substituted monomers, the compatibility with diverse functionalities as well as the physicochemical properties of a wide range of functional POx.[17-21] Early studies also revealed promising potentials of water-soluble POx,

especially of poly(2-methyl-2-oxazoline) (PMeOx) and poly(2-ethyl-2-oxazoline) (PEtOx) for biomedical applications,[22] with further important and exciting discoveries made within the last two decades.[23, 24] Numerous studies have contributed to a better understanding of their *in vitro* and *in vivo* behaviour,[25, 26] as well as their potential as drug- and gene-carriers.[4, 24, 27-32] *In vitro* studies examining the cytocompatibility and hemocompatibility of PCIEs have been predominant,[33-36] whereas immunological studies are rare. Kronek and co-workers investigated the immunological activity of PEtOx in rodent secondary cell lines and demonstrated high compatibility.[37] Furthermore, Moreadith, Viegas et al. examined the immunogenicity of their PEtOx based therapeutic in male New Zealand white rabbits. They showed that no antibodies against any component of PEtOx were developed.[38] Recently, we investigated hyperbranched PEtOx and PMeOx in comparison to PEG regarding their *in vivo* biodistribution and interaction with the murine mononuclear phagocyte system (MPS).[39] However, studies on the immunological behaviour of POx with a range of human immune cells, for example primary human immune cells from whole human blood, have not been conducted to the best of our knowledge.

In recent years, another polymer class of the PCIE family, namely poly(2-oxazine)s (POz), which comprise an additional methylene group in the backbone of each repeating unit, has gained more attention as functional polymer systems with similar but mainly unexplored potential.[40] A recent report comparing the protein absorption and cell adherence properties of different PCIE modified surfaces has further increased the interest in this polymer class.[41] Herein, planar SiO_2 surfaces were coated with PEtOx, PMeOx, poly(2-methyl-2-oxazine) (PMeOz) and PEG. Interestingly, PMeOx and PMeOz modified surfaces exhibited exceptional hydration properties and inertness, resulting in decreased cell adherence of surfaces coated with these polymers. Noteworthy, SiO_2 surfaces coated with PMeOz showed the lowest cell adherence, highlighting its low-fouling potential. Whether the low-fouling properties of PMeOz on SiO_2 surfaces translates to biological stealth properties in the more complex environment of human blood has not previously been studied.

In order for polymers to be suitable for systemic applications with extended blood circulation times, they need to possess stealth properties but also meet certain size requirements, e.g. to avoid fast renal clearance.[42] This is typically achieved through the synthesis of high molar mass polymers, or post-polymerisation processes to form polymer-based nanoparticles. To date, numerous techniques have been applied for the fabrication of POx based nanoparticles with the self-assembly of amphiphilic POx block copolymers being the predominant one.[43-45] Recently, Delaittre and co-workers prepared PEtOx containing nanostructures by reversible addition fragmentation chain-

transfer (RAFT) polymerisation induced self-assembly (PISA) using PEtOx based chain transfer agents (CTAs).[46] In general, the combination of CROP with other polymerisation techniques has received considerable attention for the fabrication of sophisticated PCIE based nano-sized materials. PCIE-based macromonomers, initiators, or CTAs have enabled the combination of CROP and reversible-deactivation radical polymerisation (RDRP) techniques.[47-49] For example, bottle brush polymers have successfully been synthesised by RAFT polymerisation of POx[50] and POz[51] macromonomers.[52] A recent study by Johnson and co-workers further extended this concept to grafting-through ring-opening metathesis polymerisations for the preparation of core cross-linked POx brush polymers.[53]

The aim of this study was to prepare core cross-linked micelles (CCMs) containing PCIE shells with different backbone and side-chain chemistries using the CROP-RDRP strategy and investigate their interaction with primary human blood immune cells. To examine the effect of chemical composition of the shell, CCMs constituting different PCIEs (PMeOx, PEtOx, PMeOz, and poly(2-ethyl-2-oxazine) (PEtOz)) of the same DP in the shell were prepared. In addition, CCMs with PEtOx shells of varying degree of polymerisation (DP), namely 50, 75, or 100, were used to gain further insight into the importance of the length of the shell-forming polymer. The library of PCIE-based CCMs was prepared in two steps; first CROP of CIEs was employed for the preparation of PCIE based CTAs, which were subsequently used in surfactant-free RAFT-mediated emulsion polymerisations. Cross-linking during the emulsion polymerisation was exploited for the synthesis of defined CCMs as determined by SEC, DLS and TEM measurements in a reproducible manner. Association studies with different primary immune cells in a whole human blood assay revealed that the chemistry and DP of the PCIE shell are crucial for the performance of the PCIE CCMs. POx were found to interact to a much lesser extent with the different immune cell populations with PMeOx CCMs demonstrating outstanding stealth properties under all conditions studied.

Materials and Methods

Materials

4-cyano-4-[(dodecylsulfanylthiocarbonyl)sulfanyl]pentanoic acid (Boron molecular), anhydrous acetonitrile (MeCN, Sigma-Aldrich), anhydrous triethylamine (NEt_3, Sigma-Aldrich), basic aluminium oxide (Sigma-Adrich), Cy5-maleimide (Lumiprobe), 2-aminoethanol (Sigma-Aldrich),

anhydrous dichloromethane (Sigma-Adrich), sodium sulfate (Sigma-Aldrich), and Barium oxide (BaO, Sigma-Aldrich) were used as received.

Azobisisobutyronitrile (AIBN, 0.2 M in toluene, Sigma-Aldrich) was recrystallised from methanol and dried *in vacuo* prior to utilization.

Methyl *p*-toluenesulfonate (MeOTos, Sigma-Adrich), 2-ethyl-2-oxazoline (EtOx, Sigma-Aldrich) and 2-methyl-2-oxazoline (MeOx, Sigma-Aldrich) were distilled to dryness over BaO prior utilisation.

Ethylene glycol dimethacrylate (EGDMA, Sigma-Aldrich) and *n*-butyl methacrylate (BMA, Sigma-Aldrich) were filtered over basic aluminium oxide prior utilisation.

2-Etyhl-2-oxazine (EtOz) and 2-methyl-2-oxazine (MeOz) were synthesised after literature procedures and distilled to dryness over BaO prior utilisation.[54]

All other chemicals were purchased from standard suppliers and used as received.

Instrumentation

^{1}H Nuclear Magnetic Resonance (^{1}H NMR) spectroscopy of all samples was carried out using a Bruker AVANCE III HD 400 MHz spectrometer using deuterated solvents obtained from Sigma-Aldrich.

Analyses of polymer solutions were performed using a Shimadzu modular system comprising a DGU-12A degasser, an SIL-20AD automatic injector, a 5.0 μm bead-size guard column (50 × 7.8 mm) followed by three KF-805L columns (300 × 8 mm, bead size: 10 μm, pore size maximum: 5000 Å), a SPD-20A ultraviolet detector, and an RID-10A differential refractive index detector. A CTO-20A oven was used to maintain the columns at 40 °C. N, N-dimethylacetamide (DMAc) with 0.03% w/v LiBr was used as the eluent where samples were run isocratically at 1 mL min^{-1}. Polystyrene standards (0.5 to 2000 kg mol^{-1}) were used for calibration. Analyte samples were filtered through 0.45 μm PTFE filters before injection. Molar mass (M_n, SEC) and dispersity (Đ) values of samples were determined on Shimadzu LabSolutions software.

Dynamic light scattering (DLS) analysis was carried out using a Malvern Zetasizer Nano ZS. All measurements were carried out at 25 °C using unfiltered polymer solutions (MQ or PBS) of 2 mg mL^{-1}.

A Tecnai T20 200 kV was used to obtain scanning transmission electron microscopy (TEM) images. TEM sample preparation was done by aliquoting (2 μL) of 1 mg mL^{-1} deposited on a

Formvar coated copper grid (GSCu100F-50, Proscitech) and allowed to dry overnight in air and at ambient temperature.

Calculation of hydrophilic-lipophilic balance (HLB)

HLB values were calculated in accordance to the Davies method depicted in equation (1).[55]

$$HLB = 7 + \sum_{i=1}^{h} H_i - l \cdot 0.475 \quad (1)$$

h: number of hydrophilic groups in the molecule

H_i: Value of the i^{th} hydrophilic groups

l: Number of the lipophilic groups in the molecule

Synthesis

Synthesis of macro CTAs

The synthesis of macro CTAs was adapted from A. Krieg et al.[47] and is exemplarily described for the preparation of $PEtOx_{50}$ CTA.

In a dry reaction vessel equipped with a stirrer bar, EtOx (2.4 g, 0.024 mol, 50 equiv.), MeOTos (0.09 g, 4.8 mmol, 1 equiv.) and anhydrous MeCN (3.48 mL) were mixed under inert conditions. The reaction vessel was sealed and heated to 80 °C for 5 h in an oil bath and then cooled to room temperature. In a separate vessel, 4-cyano-4-[(dodecylsulfanylthiocarbonyl)sulfanyl]pentanoic acid (C12-CTA, 0.16 g, 4.8 mmol, 1 equiv.) was dispersed in anhydrous MeCN (1.5 mL) under inert conditions and heated to 50 °C until the compound was completely dissolved. Subsequently, the C12-CTA solution was transferred to the polymerisation mixture by using a syringe which was purged with N_2 beforehand. Then, anhydrous triethylamine (67 µL, 4.8 mmol, 1 equiv.) was added via septum and the reaction mixture was stirred at 50 °C for 2 h, cooled to room temperature and stirred overnight. After that, the crude product was diluted with 50 mL dichloromethane and washed with 100 mL saturated aqueous $NaHCO_3$ solution twice and with brine once. The organic layer was dried over Na_2SO_4. After filtering off the salt, the solvent was evaporated under reduced

pressure until complete dryness. The product was then re-dissolved in MQ water and freeze dried to obtain the product as a yellow powder.
MeOx and MeOz containing macro CTAs were purified by dialysis (regenerated cellulose (RC), MWCO 3.5 kDa) against 1 L methanol, for five washes and then MQ water for five more washes and lyophilised to obtain the product as a yellow powder.

Synthesis of CCMs

In a reaction vessel, 100 mg macro CTA were dissolved in 1 mL MQ water in a microwave reaction vial (Biotage). In a separate vial, 1 mg AIBN was dissolved in a mixture of 19 µL ethylene glycol dimethacrylate and 49 µL butyl methacrylate. 68 µL of the monomer-initiator mixture was then carefully layered on top of the aqueous macro CTA solution. The solution was emulsified using a sonication probe (amplitude 20%, 10 sec) while cooling in an ice bath. Then, a stirrer bar was added, the vessel was sealed, and the reaction mixture was deoxygenated in an ice bath with N_2 for 15 min. Subsequently, the reaction vessel was placed in a preheated oil bath at 70 °C and stirred (100 rpm) for 4 h.
After the reaction was completed, the reaction mixture was diluted with MeOH to a total volume of 10 µL and filtered through a 0.45 µL PTFE syringe filter. Then, the crude product was purified by using Vivaspin (MWCO 100 kDa, Biostrategy) centrifuge tubes (three washes with 20 mL MeOH, then three washes with 20 mL MQ water). The solution was lyophilised to obtain the product as a yellowish powder.

Synthesis of $PEtOx_{50}$-b-BMA_{20}

The synthesis of $PEtOx_{50}$-*b*-BMA_{20} was proceeded in accordance with the CCM synthesis with the variation that 68 µL butyl methacrylate (BMA) and no ethylene glycol dimethacrylate (EGDMA) was used.

Cy5 labelling of CCMs

Reactant quantities were kept constant for all reactions, independent of the CCM used.
In a reaction vessel equipped with a stirrer bar 10 mg of CCM and 1 mg Cy5-maleimide were dissolved in 500 µL anhydrous DCM, closed with a rubber septum, and deoxygenated with N_2 in

an ice bath for 10 min. A separate vessel, containing a 10 v/v% of ethanolamine in anhydrous DCM was sealed with a septum and deoxygenated with N_2 in an ice bath for 10 min. A micro syringe was deoxygenated at the same time. Subsequently, 7 µL of the ethanolamine solution (0.7 mg ethanolamine) was transferred to the polymer-dye solution. The reaction mixture was stirred at 25 °C in the dark overnight. Then, the crude mixture was purified by preparative size-exclusion chromatography using Biobeads® S-X1 dispersed in $CHCl_3$. The solvent was removed under reduced pressure and re-dissolved in MQ. After that, the aqueous solution was lyophilised to obtain the polymer as a blue solid. Purity from free Cy5 dye determined by SEC measurements equipped with a UV detector (λ_{ex} = 646 nm).

The relative labelling efficiency of CCMs has been determined by fluorescence measurements (λ_{ex} = 646 nm; λ_{em} = 670 nm) (PEtOx$_{50}$: 2.1; PEtOx$_{75}$: 1.0; PEtOx$_{100}$: 1.1; PMeOx$_{75}$: 0.9; PMeOz$_{75}$: 4.3; PEtOz$_{75}$: 1.6; PDMAEMA: 3.5).

Determination of the cloud point temperature (T_{cp})

The T_{cp} of polymers was determined by DLS measurements.[56]
For this purpose, 1 mg of polymer was dissolved in 1 mL solvent (MQ or PBS) and filtered through 0.45 µm nylon syringe filter prior measurements. Samples were heated in shown steps for the indicated temperature range (usually 25 °C to 70°C). After heating to a certain value, the sample was equilibrated for ten seconds prior the measurement. The T_{cp} was defined as 50% between the onset and the maximum of the linear size increase. Measurements were conducted in triplicate with three runs each. Values shown represent the mean and SD.

Cell Culture

Mouse leukemic macrophage RAW 264.7 (purchased from ATCC) used in this study were tested and cleared for mycoplasma. RAW 264.7 cells were kept in Dulbecco's modified Eagle's medium (DMEM) Glutamax™ supplemented with 1 mM sodium pyruvate 10% v/v fetal bovine serum. The cells were cultured at 37 °C in a humidified incubator with 5% atmospheric CO_2. Cell counting for passaging was determined by adding 0.4% trypan blue solution to the cells in medium and using a haemocytometer.

Cell Viability

Cell viability was tested via AlamarBlue® assay. Cells were seeded the day before in 96-well plates at a density of 10 000 cells per well, leaving the outer wells empty. The cells were then incubated with polymer samples (0.04 to 5 mg mL^{-1} (0.5 to 0.004 in case of $PEtOz_{75}$ CCM) in PBS, prepared through serial dilution) and incubated at 37 °C for 24 h in a humidified incubator with 5% atmospheric CO_2. Samples were run as triplicates. After incubation, the medium was removed and a 10% v/v solution of AlamarBlue® in DMEM was added. The cells were incubated for a further 4 h at 37 °C. Cell viability was determined by measuring the fluorescence (λ_{ex} = 540 nm, λ_{em} = 590 nm). Wells incubated without cells were used as blank. Control samples were cells incubated with PBS (without polymer). The viability was calculated using the following equation

$$cell\ viability(\%) = \frac{FI\ sample - FI\ blank}{FI\ control - FI\ blank} \times 100$$

where FI = fluorescence intensity.

Healthy human donor blood

Blood was collected from healthy human donors after obtaining informed consent in accordance with University of Melbourne Human ethics approval 1443420 and the Australian National Health and Medical Research Council Statement on Ethical Conduct in Human Research. Blood was collected in Vacuette® blood collection tubes containing K2-EDTA as an anti-coagulant (Greiner Bio-One). Tubes were inverted 5 times to mix with anti-coagulant. Blood was studied within 1 h of collection. All experiments were conducted with informed consent.

Haemoglobin release assay

To assess the haemolytic activity of the CCM solutions, blood from a healthy human donor was collected as described above and centrifuged at 950 × g for 12 min. The pellet was washed three times with cold 1.5 mmol L^{-1} phosphate buffered saline (PBS, pH = 7.4). After dilution with PBS in a ratio of 1:7, aliquots of erythrocyte suspension were mixed 1:1 with the polymer solution to obtain indicated concentrations (10 and 100 µg mL^{-1}) and incubated in a water bath at 37 °C for 60 min. After centrifugation at 2400 × g for 5 min, 100 µL of the supernatant were removed and

transferred into a clear flat bottom 96 well plate. The haemoglobin release into the supernatant was determined spectrophotometrically using a microplate reader at λ_{ex} = 544 nm wavelength. Complete haemoglobin release (100%) was achieved using 1% Triton X-100 serving as positive control. Thereby, PBS served as negative control (0%). A value less than 2% haemoglobin-release rate was taken as non-haemolytic. Experiments were run in triplicates. The haemolytic activity of the CCMs was calculated by equation (2).[29]

$$\%\, Hemoglobin\ release = 100 \times \frac{(A_{sample} - A_{negative\ control})}{A_{positive\ control}} \quad (2)$$

Erythrocyte aggregation

For the examination of the erythrocyte aggregation, erythrocytes were isolated as described above. An erythrocyte suspension was mixed with the same volume of polymer solution to obtain indicated concentrations (10 and 100 µg mL^{-1}) in a clear flat bottomed 96-well plate. The cells were incubated at 37 °C for 2 h, and the absorbance was measured at λ_{ex} = 645 nm in a microplate reader. Triton X-100 (1%) was used as positive control and PBS-treated cells served as the negative control. Absorbance values of the test solutions lower than the negative control were regarded as aggregation. Experiments are the result of triplicates.

Cell association/uptake experiments

The interaction of polymers and fresh blood cells was determined using a fresh whole blood model as described previously.[57-59] Briefly, 100 µl of fresh human blood was added to 5 mL polystyrene test tubes (Falcon), capped, and incubated in a 37 ˚C water bath or on ice (4 ˚C) for 15 min. CCMs (1.0 µg) or PBS control was added to blood, mixed briefly by vortex mixer and returned to 37 ˚C or ice for 1 h. Following incubation, samples were placed on ice and erythrocytes lysed with Pharm Lyse buffer (BD Biosciences). Samples were washed twice with PBS, and cells phenotyped with a panel of anti-human antibodies in 7 fluorophores on ice for 1 h to identify the 6 major white blood cell populations. The antibody panel comprised CD3 AF700, SP34-2; CD14 APC-H7, MΦP9; CD20 BV421, 2H7; CD45 V500, HI30; CD56 PE, B159; HLA-DR PerCP Cy5.5, L243; and Lineage-1 cocktail FITC (containing CD3 SK7, CD14 MΦP9, CD16 3G8, CD19 SJ25C1, CD20 L27, CD56 NCAM16.2). All antibodies were from BD Biosciences, except CD20 (BioLegend). Samples washed three times with FACS Wash Buffer [1× PBS containing 0.5% w/v bovine serum

albumin (Sigma Aldrich) and 2 mM EDTA pH 8 (Ambion)], fixed with 1% formaldehyde and analysed by flow cytometry (LSRFortessa, BD Biosciences). Gated populations of single cells were analysed for association with Cy5-HBP (FlowJo v10), and median fluorescent index (MFI) summarized using OriginPro 2015. Representative gating strategy can be found in Figure S36.

Plasma depletion experiments

For plasma depletion experiments, 3 mL fresh blood was first diluted to 50 mL with 1× PBS and centrifuged at 950 × g, 10 min, slow brake. For the subsequent five wash steps, the supernatant was aspirated to a volume of 7.5 mL (to avoid disturbing cell pellet), before diluting to 50 mL with PBS and repeating centrifugation. At the sixth wash, the supernatant was aspirated to a final cell volume of 3 mL. Cell association/uptake was then assessed using 100 µl 'washed blood' as for fresh blood above. The supernatant protein concentration was measured at each wash using a UV-Vis spectrophotometer at λ_{ex} = 280 nm (NanoDrop 2000, ThermoScientific). Cell counts and compositions were recorded pre- and post-washing using a CELL-DYN Emerald (Abbott Diagnostics).

Results and discussion

Previously, the potential of PEtOx and PMeOx to act as surfactants for oil-in-water emulsions has been reported.[33] Based on this, the introduction of a terminal hydrophobic CTA was assumed to enhance this feature, enabling the PCIE to simultaneously act as emulsifier, and macro CTA.

Synthesis of macro CTAs

The CROP of CIEs is a versatile method to prepare tailored polymers with defined functionalities. A broad range of monomers of varying ring composition (e.g., 2-oxazolines (5-membered ring) or 2-oxazines (6-membered ring)) and 2-substituents have been reported to undergo CROP.[60] To obtain water-soluble CCMs, four short aliphatic monomers were chosen as the building blocks for the hydrophilic PCIE shell, resulting in water-soluble polymers with tailored hydrophobicity: (i) PEtOx, (ii) PMeOx, (iii) PEtOz and, (iv) PMeOz.

PCIE macro CTAs were prepared by the termination of CROP with a carboxylic acid functional CTA (Scheme 1A).[47, 48] 4-Cyano-4-[(dodecylsulfanylthiocarbonyl)sulfanyl]pentanoic acid (C12-CTA), a commercially available hydrophobic CTA, was selected for this purpose. C12-CTA has previously been used as a small molecule emulsifier for RAFT-mediated emulsion polymerisation [61] and was therefore assumed to be the ideal candidate for the preparation of amphiphilic PCIE macro CTAs. Specifically, six polymers were synthesized: (i) PEtOx$_{50}$-CTA, (ii) PEtOx$_{75}$-CTA, (iii) PEtOx$_{100}$-CTA, (iv) PMeOx$_{75}$-CTA, (v) PEtOz$_{75}$-CTA, and (vi) PMeOz$_{75}$-CTA (Table S1). With respect to size-exclusion chromatography (SEC) measurements (Figure S1, Table S1) all polymers showed narrow dispersities (Đ < 1.3). Furthermore, end-group fidelities were determined to be > 94% by proton nuclear magnetic resonance (^{1}H NMR) analysis (Table S1, Figure S2 to S7). Herein, the peak of the initiating methyl group at δ = 2.9 ppm was compared to the CH_2 group of the polymer backbone next to the terminating agent at δ = 4.1 to 4.2 ppm. The purity of the macro CTAs was confirmed by SEC measurements using a UV detector (λ_{ex} = 310 nm), which suggested complete removal of free C12-CTA.

The four chosen polymers vary in hydrophilicity (Scheme 2A) in the following order: PMeOx > PMeOz > PEtOx > PEtOz.[54] Notably, the ethyl-substituted polymers PEtOx and PEtOz possess lower critical solution temperature (LCST) behaviours.[54] Previous studies have shown that the LCST of PCIEs is dependent on their DP[62] as well as their α- and ω-end group[63]. In the case of the prepared PCIE macro CTAs, a decrease of the cloud point temperature (T_{cp}) was expected due to the hydrophobic dodecyl group. To avoid precipitation of the emulsifying macro CTA during the subsequent RAFT-mediated emulsion polymerisation, the aqueous solution behaviour of the synthesised macro CTAs was examined between 25 °C and 70 °C (Table S1) using dynamic light scattering (DLS). Within the investigated temperature range, only PEtOz$_{75}$-CTA showed a T_{cp} below the aimed RAFT polymerisation temperature of 70 °C. Unfortunately, a variation of the DP of this polymer was not possible, since a higher DP leads to a further decrease of the T_{cp} whereas a lower DP results in a lower aqueous solubility of the polymer due to the hydrophobic end-group and consequently, decreased stability of the emulsion.

In a previous study investigating POx as emulsifiers, narrowly distributed nanoparticles were obtained utilising a surfactant concentration of 100 mg mL^{-1}.[33] For this reason, the aforementioned concentration was applied for the emulsification process using PCIE macro CTAs. In addition to the general stabilisation properties of PCIEs, the hydrophobic C12-CTA end-group was expected to be most likely at the interphase of the organic and the aqueous layer, contributing to the

polymerisation process in the dispersed phase (Scheme 1B). This was also suggested by DLS measurements of an aqueous solution of the macro CTAs, which showed the formation of assembled structures (Figure S8).

Surfactant-free RAFT-mediated emulsion polymerisation

PCIE macro CTAs were dissolved in water to obtain a clear, yellowish solution. A solvent free mixture of the two monomers butyl methacrylate (BMA) and ethylene glycol dimethacrylate (EGDMA) containing azobisisobutyronitrile (AIBN) as a hydrophobic initiator was carefully layered on top of the aqueous layer before preparation of an emulsion using a sonication probe. Exemplarily, the bulk RAFT-mediated emulsion polymerisation using $PEtOx_{50}$-CTA was monitored by SEC (Figure 1) as well as ^{1}H NMR (Figure S9A and S9B) and DLS measurements (Figure S9C). Here, ^{1}H NMR measurements served the purpose to determine the linearity of the monomer conversion over time (Figure S9A), verifying controlled polymerisation which is mediated by the CTA ω-end group of the emulsifier. After a short retardation of 30 min, a typical RAFT-polymerisation pseudo first order kinetic profile was observed, with linearity shown for the first 120 min of polymerisation (Figure S9A and S9B). Due to the high complexity of the kinetics NMRs, the degree of cross-linking could not be measured by this technique. For this reason, SEC measurements were used to display the formation of CCMs.

After approximately 90 min, the polymer dispersity (Đ) increased significantly from Đ < 1.2 to Đ > 1.9 (Figure 1A), indicative of the beginning of the cross-linking reaction. After 120 min, the molar mass of the CCMs differed significantly from the macro CTA, as apparent from the appearance of a second, separated peak (Figure 1B). Notably from that time point, the CCMs increased in yield with respect to the macro CTA peak, but remained constant in terms of the polymer size and dispersity, which eventually resulted in well-defined CCMs of high molar mass (M_n = 208 kg mol^{-1}) and narrow dispersity (Đ = 1.06, Table 1). The obtained DLS data (Figure S9) supported these results by showing that the z-average size as well as the polydispersity index (PDI) of the dispersed phase decreased approximately after 60 to 90 min, indicating the beginning of the cross-linking process. From this initial study, reaction times of up to 360 min were determined to be suitable for the preparation of well-defined CCMs.

Synthesis of a library of CCMs

After initial examinations, a series of different PCIE containing CCMs was synthesised by RAFT-mediated emulsion polymerisation and characterised using SEC (Table 1).

With respect to SEC measurements (Figure 2, Table 1), all CCMs showed monomodal and narrow molecular weight distributions (Đ < 1.2), indicative of the high controllability of the cross-linking process, as further demonstrated by excellent reproducibility (Figure S10). PEtOx containing CCMs possessed molar masses of 208 kg mol^{-1} to 317 kg mol^{-1}, which increased in dependence on the DP of the macro CTA. ^{1}H NMR measurements did not allow to determine the final monomer ratios (Figure S11A), presumably due to shielding of the CCM cores by the PCIE shells.

To analyse the successful chain-extension of the macro CTA with the methacrylates, a control polymer was prepared under the same conditions as the CCMs but in the absence of cross-linker. ^{1}H NMR measurements of the purified polymer clearly showed signals of BMA (Figure S11B), suggesting the formation of a block copolymer consisting of $PEtOx_{50}$ and BMA.

Physicochemical properties of CCMs

DLS measurements were employed to determine hydrodynamic diameters (d_H, Table 1, Figure 3 and S12 to S15) and possible lower critical solutions temperature (LCST) behaviours (Table 1, Figure S18 to S21) of the CCMs. Measurements of 1 mg mL^{-1} solutions at 25 °C in ultra-pure water (MQ) revealed similar sizes (d_H < 50 nm) for all CCMs with PDIs ≤ 0.2. The only exception was the $PEtOz_{75}$ CCMs, which showed a higher d_H and a slightly larger PDI (d_H = 148 ± 27 nm, PDI = 0.27 ± 0.06). This difference in size might be attributed to the increased hydrophobic character of the polymer or possibly, a lower LCST, causing further aggregation of the CCMs. Cloud point temperature (T_{cp}) measurements of 1 mg mL^{-1} solutions were conducted (Table 1 and S1, Figures S18 to S21) to obtain information about possible LCST properties of PEtOx and PEtOz CCMs. $PEtOz_{75}$ containing CCMs displayed an exceptionally low T_{cp} (T_{cp} = 27 °C), whereas all PEtOx containing CCMs showed a T_{cp} higher than 60 °C and thus, far outside the physiological range (Table 1). The decrease in the cloud point temperature after chemical cross-linking is in accordance with previous studies.[64] DLS measurements in physiological PBS revealed only a slight impact of the T_{cp} on the presence of salt (e.g. for $PEtOx_{50}$ CCMs: $T_{cp(MQ)}$ = 69 °C, $T_{cp(PBS)}$ = 66 °C).[50]

To further understand the differences in the distribution, the PDIs of the CCMs were correlated to the hydrophilic-lipophilic balance (HLB) value (equation 1) of the macro CTAs (Figure 3C) as defined by J. T. Davies.[55] According to this, higher HLB values refer to more hydrophilic compounds. When applied to the different PCIE-based macro CTAs, a correlation between the PDI of each CCM and the HLB of the macro CTA was observed. Notably, $PEtOz_{75}$ possessed the lowest HLB value of 4 and the highest PDI of 0.27, whereas $PMeOx_{75}$ is characterised by an exceptionally high HLB value of 75 and the lowest PDI of 0.09. Furthermore, the isomers $PEtOx_{75}$ and $PMeOz_{75}$ revealed identical HLB values of 39 and, also showed very close PDI values (PDI_{PEtOx} = 0.17; PDI_{PMeOz} = 0.19). Consequently, it is suggested that the ability to form narrowly distributed CCMs can be estimated by the HLB value of the emulsifying macro CTA and is related to the relative solubility of the stabilising macro CTA in the solvent.

After initial characterisation using DLS measurements, the morphology of the CCMs was visualised using TEM (Figure 4 and S22), revealing similar sizes with a diameter of around 20 nm. The mean diameters calculated from DLS are larger than those observed from TEM images, which may be due to the hydrated PCIE shell in aqueous solution or decreased contrast of the shell. [65, 66, 67] The similarity of sizes between the CCMs make them ideal candidates for biological evaluation, correlating cellular interaction behaviours to the chemistry of the PCIE shell rather than their size.

In vitro cyto- and haemocompatibility of CCMs

Cyto- and haemocompatibility (Figures S28 and S29) of CCMs were investigated using RAW264.7 macrophages and erythrocytes from human blood, respectively. Treatment of erythrocytes with two different concentrations (10 and 100 µg mL^{-1}) of PCIE CMMs did not result in any measurable aggregation or haemoglobin release (Figure S28). Because of their potential cationic charge and high interaction with cellular membranes, poly(2-(dimethylamino)ethyl methacrylate) (PDMAEMA) containing CCMs with the same core composition as PCIE CCMs were investigated as control polymers, leading to concentration dependent haemoglobin release of 8.0 ± 0.1% (10 µg mL^{-1}) and 51.3 ± 12.9% (100 µg mL^{-1}) as well as erythrocyte aggregation. Similarly, the AlamarBlue™ assay verified the high cytotoxicity of PDMAEMA CCMs at all tested concentrations, while none of the low-fouling CCMs affected the cell viability of RAW264.7 macrophages (Figure S29). Interestingly, treatment of cells with high concentrations of CCMs other than PDMAEMA led to an increase of cell growth compared to the PBS control: $PEtOx_{50}$

(131%), $PEtOx_{75}$ (133%), $PEtOx_{100}$ (134%), $PMeOx_{75}$ (149%), $PMeOz_{75}$ (151%) and PEtOz (123%) CCMs (Figure S29), which is in agreement with previous studies.[24, 32, 34, 35, 68] Noteworthy, the investigated concentrations of the polymers are relatively high, exceeding commonly applied polymer concentrations of *in vivo* studies. In the following study, CCMs were investigated regarding their interaction with immune cells at a polymer concentration of 10 µg mL^{-1} at which *in vitro* cell growth appeared to be similar to the control (Figure S29C and S29D).

Immune cell interaction of CCMs in whole human blood

After verification of their general cyto- and haemocompatibility, the CCMs were investigated regarding their association with primary immune cells. The bloodstream of a mammal is a complex environment, which is difficult to model due to the existence of multiple cell types and a complex mix of plasma proteins, lipids, and sugars. To study a physiologically-relevant complex cellular environment, a whole human blood assay, an assay recently shown to deliver results which are well correlated with *in vivo* blood clearance experiments in mice, was utilised.[69] Three different conditions were investigated: (i) the interaction of CCMs with whole human blood, (ii) the interaction of CCMs with plasma-depleted blood, and (iii) the interaction of protein pre-incubated CCMs with plasma-depleted blood. The whole blood experiment provides information about immune cell association in a biologically relevant environment.[69] In contrast, plasma depletion experiments allow to study the effect of the protein-corona on the association of CCMs to different immune cells.

To reveal the effect of polymer shell size and composition on immune cell interactions, the different PCIE containing CCMs were studied. Shells consisting of PMeOx, PEtOx, PMeOz, and PEtOz (Scheme 2) were believed to provide insights in the importance of the composition of the PCIE, while PEtOx shells of varying DP (50, 75, or 100) were used to reveal the impact of the length of the shell-forming low fouling polymer. Furthermore, a CCM with cationic PDMAEMA in the shell was used as a high fouling low-stealth control, known for its high cellular interaction.[70, 71]

First, all CCMs were incubated for 1 h at 37 °C in whole human blood. Flow cytometry was employed to examine the cellular interactions of CCMs (Figures 5 and S30 to S32, Table S3) simultaneously with six different immune cells within blood: (i) granulocytes (phagocytic), (ii) monocytes (phagocytic), (iii) B cells, (iv) dendritic cells (DCs), (v) natural killer cells (NKs), and

(vi) T cells. PMeOx based CCMs demonstrated remarkably low interactions with all investigated immune cells (<10%) in whole blood, which was significantly lower than the interaction of the high-fouling PDMAEMA control CCMs with these cells ($p < 0.005$) (Figure 5). In contrast, PEtOx containing CCMs revealed a higher association with immune cells, which was significantly enhanced for phagocytic granulocytes, and monocytes, and B cells (all $p < 0.005$) when compared to PMeOx CCMs. In addition, both POz CCMs showed enhanced cellular interactions with primary immune cells compared to PMeOx and PEtOx ($p < 0.005$). Surprisingly, PMeOz, which is more hydrophilic than PEtOx, showed very high immune cell associations in whole blood, which is in contrast to the recent study on the low-fouling behaviour of PMeOz-coated planar surfaces, where very low protein absorption and cellular adhesion was observed.[41] This discrepancy might be explained by the different experimental setup of using primary human cells as well as differences in the investigated material. The current results suggest an impact of both, the side-chain and the backbone chemistry of PCIEs on the interaction of CCMs with immune cells.

The size of the CCM shell is likely to influence the stealth properties as shown for PEG-coated gold nanoparticles[72] but this effect has not yet been studies for PCIEs. Here, the relevance of the hydrodynamic volume of the shell polymer, which is related to the DP of the PCIE, was investigated with PEtOx CCMs serving as the model system. Cellular associations with the phagocytic granulocytes and monocytes as well as B cells were found to be dependent on the DP of the shell forming PEtOx (Figure S30, Table S3). PEtOx CCM interaction was significantly lower ($p < 0.0005$) than the PDMAEMA CCMs control in all cases. $PEtOx_{100}$ containing CCMs showed the lowest values of cellular interaction amongst the investigated PEtOx CCMs of different shell size. Cellular interaction of all PEtOx containing CCMs as well as the PDMAEMA CCMs with NKs and T cells was very low (<10%), which is in accordance with previously reported results.[73] However, the cellular interaction of PEtOx containing CCMs was significantly lower than the PDMAEMA CCMs ($p < 0.0005$). These results highlight the importance of the DP of the stealth polymer used for the nanoparticle shell and illustrate that longer low-fouling shell polymers allow to further reduce immune cell associations. The recognition of polymer nanoparticles by cells is dictated by different moieties, such as chirality, hydrogen bonding, hydrophobic interactions, or its (surface) charge.[74] In addition, the incorporation of specific targeting ligands into the nanoparticle shell can be utilised to trigger interactions with cellular receptors, and thus, increase the cellular specificity.[75] However, a low degree of protein association to the stealth material itself is essential for the mechanistic understanding of immune cell recognition and uptake and, therefore, is of major

importance to evaluate. Previous studies on well-established PEGylated systems have revealed the importance of the protein-corona for cellular association. It has been shown that not only a general protein corona impacts the stealth properties of these nanoparticles, but the type of proteins in the corona is important for cellular interactions.[72, 76-78] Although we comprehensively studied the general immune cell interaction of novel PCIE CCMs in physiologically relevant human cell environments, further work on the influence of the protein corona on these nanoparticles is warranted.

To further determine the stealth characteristics of the CCMs and the impact of protein interaction on the cellular association, experiments with plasma-free human blood were conducted (Scheme 2). First, CCMs were pre-incubated for 1 h in either PBS or human serum (100 μg mL^{-1}) at 37 °C. After that, CCMs were incubated with plasma-free blood, which was obtained through multiple washing cycles to replace the plasma of the whole blood with PBS.[73] The same conditions as for the whole human blood study were employed and PDMAEMA CCMs were used as control (Figures 6 and S33 to S35, Tables S4 and S4). Notably, high cellular associations (≥ 80%) of PDMAEMA CCMs was observed for all six analysed human blood immune cell types, most likely due to their cationic charges and increased interaction with the slightly negatively charged cell membranes in the absence of plasma proteins (Figures 6 and S33, Table S4). Upon the incubation with plasma proteins, the cellular interaction of PDMAEMA CCMs was decreased, likely due to high electrostatic interaction with plasma proteins covering the cationic charges of the CCMs.[29, 70]

In contrast to the PDMAEMA CCMs, under plasma-free conditions both PMeOx and PEtOx CCMs showed only marginal cellular association with the investigated cell lines (≤ 1%), whereas the POz equivalents, PMeOz and PEtOz, showed higher cellular interaction. Interestingly, granulocytes and monocytes incubated with PMeOz CCMs possessed 40.7 ± 15.7%, and 93.6 ± 2.5%, respectively, of their cell population positive (Figure 6A and 6B, Table S4). This high cellular interaction is likely caused by a weak shielding of the hydrophobic core by the low-fouling shell.[79] Due to the high flexibility of the POz backbone in combination with the low steric hinderance of the methyl side-chain, the hydrophobic core might be more accessible.

Overall, removal of plasma proteins led to decreased immune cell association for most investigated PCIE CCMs when compared to incubation with whole blood. PMeOx CCMs revealed strikingly low association independent on the presence of plasma proteins. For this reason, additional protein-corona formation experiments were conducted. CCMs pre-incubated with human plasma before

incubation with plasma-free blood were expected to provide information about the effect of a protein-corona formation on the CCMs and its impact on the cellular interactions with different immune cells (Figure 6, Table S5). While PMeOz and PEtOz CCMs showed an increase of cellular association with granulocytes, monocytes, B cells and DCs (Figure 5A to 5D), no increased cellular interaction with NKs and T cells was observed (Figure 5E and 5F). No significant increase for POx materials after incubation with plasma was recorded except for the interaction of $PEtOx_{75}$ with B cells ($p < 0.0005$, Figure 5C). In the case of all other examined cell types, the difference in cell association of plasma incubated POx was not significantly different to those incubated in PBS.

By evaluating the effect of side-chain and backbone chemistry of the low-fouling shell, POx appear superior to POz in case of the presented amphiphilic CCM system. PMeOx containing CCMs reveal very low cellular associations with all examined immune cells in plasma-containing as well as plasma-free blood. The negligible cellular association of PMeOx CCMs in the presence and absence of plasma proteins suggested high stealth properties of this system. We assume that the increased hydrophilicity of the PMeOx methyl side-chain in combination with the decreased alkyl length in each repeating unit of the POx backbone compared to the POz backbone leads to greater hydration of the CCM shell and, consequently, negligible protein interactions.[41,80]

To investigate the effect of the CCMs shell size on protein adsorption, PEtOx CCMs with different DP were compared. Noteworthy, when no plasma proteins are present, PEtOx containing CCMs did not show cell associations higher than 1% in any of the investigated cell lines (Figure S33, Table S4). To further investigate the stealth properties of PEtOx CCMs and its dependence on the hydrodynamic volume of the CCM shell, PEtOx CCMs were pre-incubated in human plasma before incubation with plasma-free blood, leading to enhanced cellular association with B cells (Figure 33, Table S5). In particular, the interaction with B cells increased significantly for $PEtOx_{50}$ and $PEtOx_{75}$ CCMs ($p < 0.0005$), but less statistically relevant in the case of $PEtOx_{100}$ CCM ($p < 0.005$) (Figure S33C). Additionally, only $PEtOx_{50}$ CCM showed a significant increase of association with monocytes ($p < 0.005$, Figure S33B). The other cells did not display significant relevant increase in association with other PEtOx CCMs. However, it is noteworthy to mention that the amount of cyanine-5 (Cy5) positive cells increased upon incubation of CCMs with plasma, showing the following trend: $PEtOx_{50} > PEtOx_{75} > PEtOx_{100}$ (Table S5). These results verify the important role the DP plays in the low-fouling shell polymer, where longer low-fouling shell-polymers have an increased capability to reduce the interaction of the hydrophobic core with plasma proteins.[81] Consequently, we speculate that the hydrodynamic volume of the linear shell-

forming polymer, which depends on its DP, is crucial for the performance of amphiphilic CCMs in a physiological environment. Furthermore, pre-incubation in human plasma led almost exclusively to B cell association while the association with other immune cells remained below 10%, indicating potential of these CCMs for the specific delivery to B cells in the future.

Conclusion and outlook

Core crosslinked PCIE micelles (CCMs) were synthesised through a combination of CROP and surfactant-free RAFT-mediated emulsion polymerisation. Using this approach, different PCIE (PMeOx, PEtOx, PMeOz, PEtOz) macro CTAs were prepared and crosslinked in emulsion, which yielded defined CCMs with different hydrophilic PCIE shells but comparable diameters. After the cytocompatibility and hemocompatibility of all CCMs was confirmed, their stealth properties were evaluated with a whole human blood assay. Overall, cellular associations with immune cells in human blood increased in the order PMeOx < PEtOx < PMeOz < PEtOz, highlighting the exceptional stealth properties of PMeOx CCMs. Importantly, PMeOx CCMs were the only material that showed less than 10% Cy5-positive cells for each investigated immune cell population (granulocytes, monocytes, B cells, dendritic cells, natural killer cells, T cells). Noteworthy, negligible differences between cell associations of POx CCMs in the presence or absence of plasma proteins indirectly suggested low protein adsorption to the surfaces of these CCMs. The increase of the DP and, consequently, the hydrodynamic volume, of the CCMs shell represents an important key factor to further improve the performance of CCMs.

In summary, our results provide an in-depth insight into the interactions of PCIE based CCMs with immune cells in whole human blood. The direct comparison of the four most prominent water-soluble POx and POz revealed the outstanding behaviour of PMeOx CCMs, further emphasising the enormous potential of PMeOx as next generation stealth material for biomedical applications.

Acknowledgements

K.K. gratefully acknowledges the award of an ARC Future Fellowship (FT190100572) from the Australian Research Council. M.N.L. acknowledges the Alexander von Humboldt Foundation for financial support and K.J.T. and S.J.K. acknowledge the NHMRC for fellowship support

(APP1148582, APP1136322). This work was carried out -in part- within the Australian Research Council Centre of Excellence in Convergent Bio-Nano Science and Technology (Project No. CE140100036). The authors acknowledge the use of instruments and scientific and technical assistance at the Monash Centre for Electron Microscopy, a Node of Microscopy Australia. The authors acknowledge the use of the facilities and the assistance of Dr Timothy Williams, Dr Yu (Emily) Chen and Dr Russel King at the Monash Centre for Electron Microscopy.

Conflict of interest

The authors declare no conflict of interest.

Ethics approval and consent to participate

Blood was collected from healthy human donors after obtaining informed consent in accordance with University of Melbourne Human ethics approval 1443420 and the Australian National Health and Medical Research Council Statement on Ethical Conduct in Human Research. All experiments were conducted with informed consent.

Availability of data and material

Additional experimental processed data to reproduce these experiments can be found in the supplementary information.

Consent for publication

All authors give their consent for publication.

References

[1] M. Elsabahy and K. L. Wooley, *Chem. Soc. Rev.*, **2013**, *42*, 5552-5576. doi: 10.1039/C3CS60064E

[2] M. A. Dobrovolskaia and S. E. McNeil, *Nat. Nanotechnol.*, **2007**, *2*, 469-478. doi: 10.1038/nnano.2007.223

[3] O. Sedlacek, B. D. Monnery, J. Mattova, J. Kucka, J. Panek, O. Janouskova, A. Hocherl, B. Verbraeken, M. Vergaelen, M. Zadinova, R. Hoogenboom and M. Hruby, *Biomaterials*, **2017**, *146*, 1-12. doi: 10.1016/j.biomaterials.2017.09.003

[4] K. L. Eskow Jaunarajs, D. G. Standaert, T. X. Viegas, M. D. Bentley, Z. Fang, B. Dizman, K. Yoon, R. Weimer, P. Ravenscroft and T. H. Johnston, *Mov. Disord.*, **2013**, *28*, 1675-1682. doi: 10.1002/mds.25625

[5] J. Kopeček, *Adv. Drug Deliv. Rev.*, **2013**, *65*, 49-59. doi: 10.1016/j.addr.2012.10.014

[6] K. Knop, R. Hoogenboom, D. Fischer and U. S. Schubert, *Angew. Chem., Int. Ed.*, **2010**, *49*, 6288-6308. doi: 10.1002/anie.200902672

[7] M. Barz, R. Luxenhofer, R. Zentel and M. J. Vicent, *Polym. Chem.*, **2011**, *2*, 1900-1918. doi: 10.1039/C0PY00406E

[8] J. J. F. Verhoef, J. F. Carpenter, T. J. Anchordoquy and H. Schellekens, *Drug Discov.*, **2014**, *19*, 1945-1952. doi: 10.1016/j.drudis.2014.08.015

[9] A. S. Abu Lila, H. Kiwada and T. Ishida, *J. Controlled Release*, **2013**, *172*, 38-47. doi: 10.1016/j.jconrel.2013.07.026

[10] S. Abbina and A. Parambath, in *Eng. Biomater. Drug Delivery Syst.*, ed. A. Parambath, Woodhead Publishing, 2018, 363-376. doi: 10.1016/B978-0-08-101750-0.00014-3

[11] M. Talelli, C. J. F. Rijcken, C. F. van Nostrum, G. Storm and W. E. Hennink, *Adv. Drug Deliv. Rev.*, **2010**, *62*, 231-239. doi: doi.org/10.1016/j.addr.2009.11.029

[12] Y. Yu, W. Xu, X. Huang, X. Xu, R. Qiao, Y. Li, F. Han, H. Peng, T. P. Davis, C. Fu and A. K. Whittaker, *ACS Macro Lett.*, **2020**, *9*, 799-805. doi: 10.1021/acsmacrolett.0c00291

[13] T. G. Bassiri, A. Levy and M. Litt, *J. Polym. Sci., Part B: Polym. Lett.*, **1967**, *5*, 871-879. doi: 10.1002/pol.1967.110050927

[14] T. Kagiya, S. Narisawa, T. Maeda and K. Fukui, *J. Polym. Sci., Part B: Polym. Lett.*, **1966**, *4*, 441-445. doi: 10.1002/pol.1966.110040701

[15] W. Seeliger, E. Aufderhaar, W. Diepers, R. Feinauer, R. Nehring, W. Thier and H. Hellmann, *Angew. Chem., Int. Ed.*, **1966**, *5*, 875-888. doi: 10.1002/anie.196608751

[16] D. A. Tomalia and D. P. Sheetz, *J. Polym. Sci., Part A: Polym. Chem.*, **1966**, *4*, 2253-2265. doi: 10.1002/pol.1966.150040919

[17] K. Kempe, E. F. J. Rettler, R. M. Paulus, A. Kuse, R. Hoogenboom and U. S. Schubert, *Polymer*, **2013**, *54*, 2036-2042. doi: 10.1016/j.polymer.2013.01.016

[18] H. M. L. Lambermont-Thijs, M. W. M. Fijten, A. J. van der Linden, B. M. van Lankvelt, M. M. Bloksma, U. S. Schubert and R. Hoogenboom, *Macromolecules*, **2011**, *44*, 4320-4325. doi: 10.1021/ma200426y

[19] H. M. L. Lambermont-Thijs, M. J. H. C. Jochems, R. Hoogenboom and U. S. Schubert, *J. Polym. Sci., Part A: Polym. Chem.*, **2009**, *47*, 6433-6440. doi: 10.1002/pola.23683

[20] K. Kempe, S. Jacobs, H. M. L. Lambermont-Thijs, M. M. W. M. Fijten, R. Hoogenboom and U. S. Schubert, *Macromolecules*, **2010**, *43*, 4098-4104. doi: 10.1021/ma9028536

[21] K. Kempe, M. Lobert, R. Hoogenboom and U. S. Schubert, *J. Polym. Sci., Part A: Polym. Chem.*, **2009**, *47*, 3829-3838. doi: 10.1002/pola.23448

[22] S. Zalipsky, C. B. Hansen, J. M. Oaks and T. M. Allen, *J. Pharm. Sci.*, **1996**, *85*, 133-137. doi: 10.1021/js9504043

[23] R. Luxenhofer, Y. Han, A. Schulz, J. Tong, Z. He, A. V. Kabanov and R. Jordan, *Macromol. Rapid Commun.*, **2012**, *33*, 1613-1631. doi: 10.1002/marc.201200354

[24] T. Lorson, M. M. Lübtow, E. Wegener, M. S. Haider, S. Borova, D. Nahm, R. Jordan, M. Sokolski-Papkov, A. V. Kabanov and R. Luxenhofer, *Biomaterials*, **2018**, *178*, 204-280. doi: 10.1016/j.biomaterials.2018.05.022

[25] J. Kronek, Z. Kroneková, J. Lustoň, E. Paulovičová, L. Paulovičová and B. Mendrek, *J. Mater. Sci.: Mater. Med.*, **2011**, *22*, 1725-1734. doi: 10.1007/s10856-011-4346-z

[26] L. wyffels, T. Verbrugghen, B. D. Monnery, M. Glassner, S. Stroobants, R. Hoogenboom and S. Staelens, *J. Controlled Release*, **2016**, *235*, 63-71. doi: 10.1016/j.jconrel.2016.05.048
[27] A. B. Cook, R. Peltier, J. Zhang, P. Gurnani, J. Tanaka, J. A. Burns, R. Dallmann, M. Hartlieb and S. Perrier, *Polym. Chem.*, **2019**, *10*, 1202-1212. doi: 10.1039/C8PY01648H
[28] B. S. Kim, H. J. Kim, S. Osawa, K. Hayashi, K. Toh, M. Naito, H. S. Min, Y. Yi, I. C. Kwon, K. Kataoka and K. Miyata, *ACS Biomater. Sci. Eng.*, **2019**, *5*, 5770-5780. doi: 10.1021/acsbiomaterials.9b00384
[29] M. N. Leiske, F. H. Sobotta, F. Richter, S. Hoeppener, J. C. Brendel, A. Traeger and U. S. Schubert, *Biomacromolecules*, **2017**, *19*, 748-760. doi: 10.1021/acs.biomac.7b01535
[30] M. M. Lübtow, L. Hahn, M. S. Haider and R. Luxenhofer, *J. Am. Chem. Soc.*, **2017**, *139*, 10980-10983. doi: 10.1021/jacs.7b05376
[31] D. Hoelzer, M. N. Leiske, M. Hartlieb, T. Bus, D. Pretzel, S. Hoeppener, K. Kempe, R. Thierbach and U. S. Schubert, *Oncotarget*, **2018**, *9*, 22316. doi: 10.18632/oncotarget.24806
[32] M. M. Lübtow, L. C. Nelke, J. Seifert, J. Kühnemundt, G. Sahay, G. Dandekar, S. L. Nietzer and R. Luxenhofer, *J. Controlled Release*, **2019**, *303*, 162-180. doi: 10.1016/j.jconrel.2019.04.014
[33] M. N. Leiske, A.-K. Trützschler, S. Armoneit, P. Sungur, S. Hoeppener, M. Lehmann, A. Traeger and U. S. Schubert, *J. Mater. Chem. B*, **2017**, *5*, 9102-9113. doi: 10.1039/C7TB02443F
[34] M. Bauer, S. Schroeder, L. Tauhardt, K. Kempe, U. S. Schubert and D. Fischer, *J. Polym. Sci., Part A: Polym. Chem.*, **2013**, *51*, 1816-1821. doi: 10.1002/pola.26564
[35] M. Bauer, C. Lautenschlaeger, K. Kempe, L. Tauhardt, U. S. Schubert and D. Fischer, *Macromol. Biosci.*, **2012**, *12*, 986-998. doi: 10.1002/mabi.201200017
[36] Z. Kroneková, T. Lorson, J. Kronek and R. Luxenhofer, *ChemRxiv*, **2018**, doi: 10.26434/chemrxiv.5793990.v1
[37] J. Kronek, Z. Kroneková, J. Lustoň, E. Paulovičová, L. Paulovičová and B. Mendrek, *J. Mater. Sci.: Mater. Med.*, **2011**, *22*, 1725-1734. doi: 10.1007/s10856-011-4346-z
[38] R. W. Moreadith, T. X. Viegas, M. D. Bentley, J. M. Harris, Z. Fang, K. Yoon, B. Dizman, R. Weimer, B. P. Rae, X. Li, C. Rader, D. Standaert and W. Olanow, *Eur. Polym. J.*, **2017**, *88*, 524-552. doi: 10.1016/j.eurpolymj.2016.09.052
[39] J. Humphries, D. Pizzi, S. E. Sonderegger, N. L. Fletcher, Z. H. Houston, C. A. Bell, K. Kempe and K. J. Thurecht, *Biomacromolecules*, **2020**, *21*, 3318-3331. doi: 10.1021/acs.biomac.0c00765
[40] M. M. Bloksma, U. S. Schubert and R. Hoogenboom, *Macromol. Rapid Commun.*, **2011**, *32*, 1419-1441. doi: 10.1002/marc.201100138
[41] G. Morgese, B. Verbraeken, S. N. Ramakrishna, Y. Gombert, E. Cavalli, J.-G. Rosenboom, M. Zenobi-Wong, N. D. Spencer, R. Hoogenboom and E. M. Benetti, *Angew. Chem., Int. Ed.*, **2018**, *57*, 11667-11672. doi: 10.1002/anie.201805620
[42] H. S. Choi, W. Liu, P. Misra, E. Tanaka, J. P. Zimmer, B. I. Ipe, M. G. Bawendi and J. V. Frangioni, *Nat. Biotechnol.*, **2007**, *25*, 1165-1170. doi: 10.1038/nbt1340
[43] J. P. Rao and K. E. Geckeler, *Prog. Polym. Sci.*, **2011**, *36*, 887-913. doi: 10.1016/j.progpolymsci.2011.01.001
[44] N. t. Brummelhuis and H. Schlaad, *Polym. Chem.*, **2011**, *2*, 1180-1184. doi: 10.1039/C1PY00002K
[45] M. Hartlieb, T. Bus, J. Kübel, D. Pretzel, S. Hoeppener, M. N. Leiske, K. Kempe, B. Dietzek and U. S. Schubert, *Bioconjugate Chem.*, **2017**, *28*, 1229-1235. doi: 10.1021/acs.bioconjchem.7b00067
[46] D. Le, F. Wagner, M. Takamiya, I. L. Hsiao, G. Gil Alvaradejo, U. Strähle, C. Weiss and G. Delaittre, *Chem. Commun.*, **2019**, *55*, 3741-3744. doi: 10.1039/C9CC00407F
[47] A. Krieg, C. Weber, R. Hoogenboom, C. R. Becer and U. S. Schubert, *ACS Macro Lett.*, **2012**, *1*, 776-779. doi: 10.1021/mz300128p
[48] A.-K. Trützschler, M. N. Leiske, M. Strumpf, J. C. Brendel and U. S. Schubert, *Macromol. Rapid Commun.*, **2019**, *40*, 1800398. doi: 10.1002/marc.201800398
[49] B. A. Drain and C. R. Becer, *Eur. Polym. J.*, **2019**, *119*, 344-351. doi: 10.1016/j.eurpolymj.2019.07.047

[50] C. Weber, C. R. Becer, R. Hoogenboom and U. S. Schubert, *Macromolecules*, **2009**, *42*, 2965-2971. doi: 10.1021/ma8028437
[51] T. Klein, J. Parkin, P. A. J. M. de Jongh, L. Esser, T. Sepehrizadeh, G. Zheng, M. De Veer, K. Alt, C. E. Hagemeyer, D. M. Haddleton, T. P. Davis, M. Thelakkat and K. Kempe, *Macromol. Rapid Commun.*, **2019**, *40*, 1800911. doi: 10.1002/marc.201800911
[52] D. Pizzi, J. Humphries, J. P. Morrow, N. L. Fletcher, C. A. Bell, K. J. Thurecht and K. Kempe, *Eur. Polym. J.*, **2019**, *121*, 109258. doi: 10.1016/j.eurpolymj.2019.109258
[53] G. G. Alvaradejo, H. V. T. Nguyen, P. Harvey, N. M. Gallagher, D. Le, M. F. Ottaviani, A. Jasanoff, G. Delaittre and J. A. Johnson, *ACS Macro Lett.*, **2019**, *8*, 473-478. doi: 10.1021/acsmacrolett.9b00016
[54] M. M. Bloksma, R. M. Paulus, H. P. C. van Kuringen, F. van der Woerdt, H. M. L. Lambermont-Thijs, U. S. Schubert and R. Hoogenboom, *Macromol. Rapid Commun.*, **2012**, *33*, 92-96. doi: 10.1002/marc.201100587
[55] J. Davies, *Proc. 2nd Intern. Congr. Surface Activity, Butterworths Scientific Publication, London*, **1957**, *426*.
[56] Q. Zhang, C. Weber, U. S. Schubert and R. Hoogenboom, *Mater. Horiz.*, **2017**, *4*, 109-116. doi: 10.1039/C7MH00016B
[57] J. Cui, R. De Rose, K. Alt, S. Alcantara, B. M. Paterson, K. Liang, M. Hu, J. J. Richardson, Y. Yan, C. M. Jeffery, R. I. Price, K. Peter, C. E. Hagemeyer, P. S. Donnelly, S. J. Kent and F. Caruso, *ACS Nano*, **2015**, *9*, 1571-1580. doi: 10.1021/nn5061578
[58] R. De Rose, A. N. Zelikin, A. P. R. Johnston, A. Sexton, S.-F. Chong, C. Cortez, W. Mulholland, F. Caruso and S. J. Kent, *Adv. Mater.*, **2008**, *20*, 4698-4703. doi: 10.1002/adma.200801826
[59] S. K. Mann, A. Dufour, J. J. Glass, R. De Rose, S. J. Kent, G. K. Such and A. P. R. Johnston, *Polym. Chem.*, **2016**, *7*, 6015-6024. doi: 10.1039/C6PY01332E
[60] K. Kempe, *Macromol. Chem. Phys.*, **2017**, *218*, 1700021. doi: doi:10.1002/macp.201700021
[61] J. Zhou, H. Yao and J. Ma, *Polym. Chem.*, **2018**, *9*, 2532-2561. doi: 10.1039/C8PY00065D
[62] C. Weber, R. Hoogenboom and U. S. Schubert, *Prog. Polym. Sci.*, **2012**, *37*, 686-714. doi: 10.1016/j.progpolymsci.2011.10.002
[63] S. Huber, N. Hutter and R. Jordan, *Colloid Polym. Sci.*, **2008**, *286*, 1653-1661. doi: 10.1007/s00396-008-1942-7
[64] A. Kowalczuk, J. Kronek, K. Bosowska, B. Trzebicka and A. Dworak, *Polym. Int.*, **2011**, *60*, 1001-1009. doi: 10.1002/pi.3103
[65] R. Szatanek, M. Baj-Krzyworzeka, J. Zimoch, M. Lekka, M. Siedlar and J. Baran, *Int. J. Mol. Sci.*, **2017**, *18*, 1153. doi:
[66] V. G. Deepagan, M. N. Leiske, N. L. Fletcher, D. Rudd, T. Tieu, N. Kirkwood, K. J. Thurecht, K. Kempe, N. H. Voelcker and A. Cifuentes-Rius, *Nano Letters*, **2021**, *21*, 476-484 doi: 10.1021/acs.nanolett.0c03930
[67] E. Gardey, F. H. Sobotta, S. Hoeppener, T. Bruns, A. Stallmach and J. C. Brendel, *Biomacromolecules*, **2020**, *21*, 1393-1406. doi: 10.1021/acs.biomac.9b01656
[68] R. Luxenhofer, G. Sahay, A. Schulz, D. Alakhova, T. K. Bronich, R. Jordan and A. V. Kabanov, *J. Controlled Release*, **2011**, *153*, 73-82. doi: 10.1016/j.jconrel.2011.04.010
[69] A. J. Sivaram, A. Wardiana, S. Alcantara, S. E. Sonderegger, N. L. Fletcher, Z. H. Houston, C. B. Howard, S. M. Mahler, C. Alexander and S. J. Kent, *ACS Nano*, **2020**, *14*, 13739-13753. doi: 10.1021/acsnano.0c06033
[70] S. Agarwal, Y. Zhang, S. Maji and A. Greiner, *Mater. Today*, **2012**, *15*, 388-393. doi: 10.1016/S1369-7021(12)70165-7
[71] L. Chen, J. J. Glass, R. De Rose, C. Sperling, S. J. Kent, Z. H. Houston, N. L. Fletcher, B. E. Rolfe and K. J. Thurecht, *ACS Appl. Bio Mater.*, **2018**, *1*, 756-767. doi: 10.1021/acsabm.8b00220
[72] C. D. Walkey, J. B. Olsen, H. Guo, A. Emili and W. C. W. Chan, *J. Am. Chem. Soc.*, **2012**, *134*, 2139-2147. doi: 10.1021/ja2084338

[73] J. J. Glass, L. Chen, S. Alcantara, E. J. Crampin, K. J. Thurecht, R. De Rose and S. J. Kent, *ACS Macro Lett.*, **2017**, *6*, 586-592. doi: 10.1021/acsmacrolett.7b00229
[74] T. Sun, G. Qing, B. Su and L. Jiang, *Chem. Soc. Rev.*, **2011**, *40*, 2909-2921. doi: 10.1039/C0CS00124D
[75] M. Elsabahy and K. L. Wooley, *Chem. Soc. Rev.*, **2012**, *41*, 2545-2561. doi: 10.1039/C2CS15327K
[76] T. Cedervall, I. Lynch, S. Lindman, T. Berggård, E. Thulin, H. Nilsson, K. A. Dawson and S. Linse, *Proceedings of the National Academy of Sciences*, **2007**, *104*, 2050-2055. doi: 10.1073/pnas.0608582104
[77] M. N. Gupta and I. Roy, *Molecular pharmaceutics*, **2020**, *17*, 725-737. doi:
[78] S. Schöttler, G. Becker, S. Winzen, T. Steinbach, K. Mohr, K. Landfester, V. Mailänder and F. R. Wurm, *Nat. Nanotechnol.*, **2016**, *11*, 372-377. doi: 10.1038/nnano.2015.330
[79] N. F. Steinmetz and M. Manchester, *Biomacromolecules*, **2009**, *10*, 784-792. doi: 10.1021/bm8012742
[80] O. Sedlacek and R. Hoogenboom, *Advanced Therapeutics*, **2020**, *3*, 1900168. doi: 10.1002/adtp.201900168
[81] A. Runser, D. Dujardin, P. Ernst, A. S. Klymchenko and A. Reisch, *ACS Appl. Mater. Interfaces*, **2020**, *12*, 117-125. doi: 10.1021/acsami.9b15396

Tables and Figures

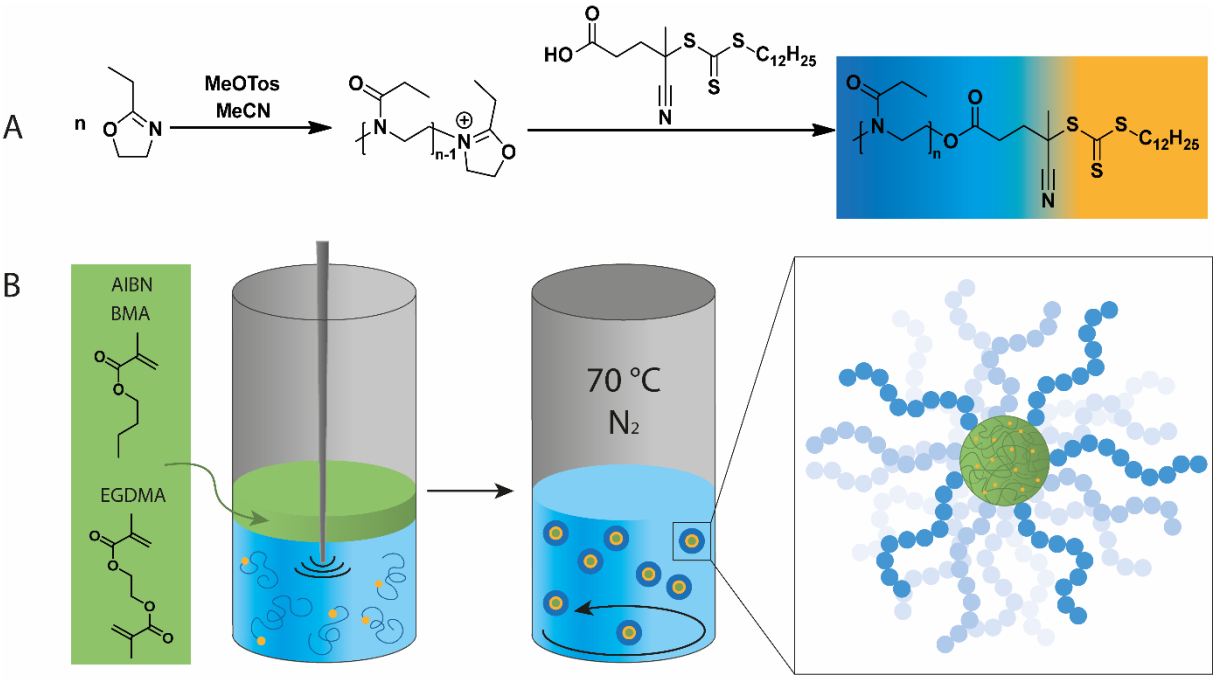

Scheme 1. Preparation of CCMs through a combination of CROP and surfactant-free RAFT-mediated emulsion polymerisation. (A) Macro CTA synthesis: CROP of CIE, followed by termination of the living polymer chain with a C12-CTA. The introduction of the ω-C12 group renders the polymer amphiphilic, which enables its use as surfactant for the following emulsion polymerisation. (B) Surfactant-free RAFT-mediated emulsion polymerisation: Macro CTAs are dissolved in water and an organic layer containing the monomer BMA, the crosslinker EGDMA and the radical initiator AIBN is carefully applied as the top layer. Both layers are emulsified using a sonication probe before sealing the reaction vessel with a rubber septum, deoxygenation, and polymerisation at 70 °C.

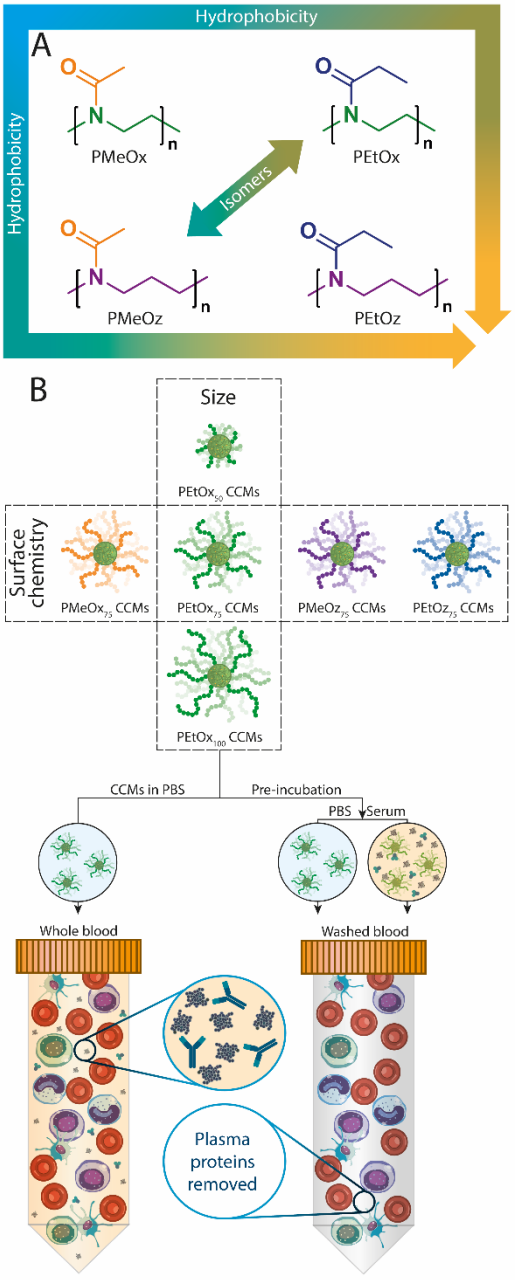

Scheme 2. A) Shell forming water soluble PCIEs used in this study. Arrows from blue to yellow indicate increasing hydrophobicity of polymers. B) CCMs were incubated for 1 h in fresh whole human blood (left) or "washed blood" (right) that had plasma replaced by PBS. Cells were phenotyped using fluorescent monoclonal antibodies before cell association was examined by flow cytometry. Note: Cell size and compositions are not to scale.

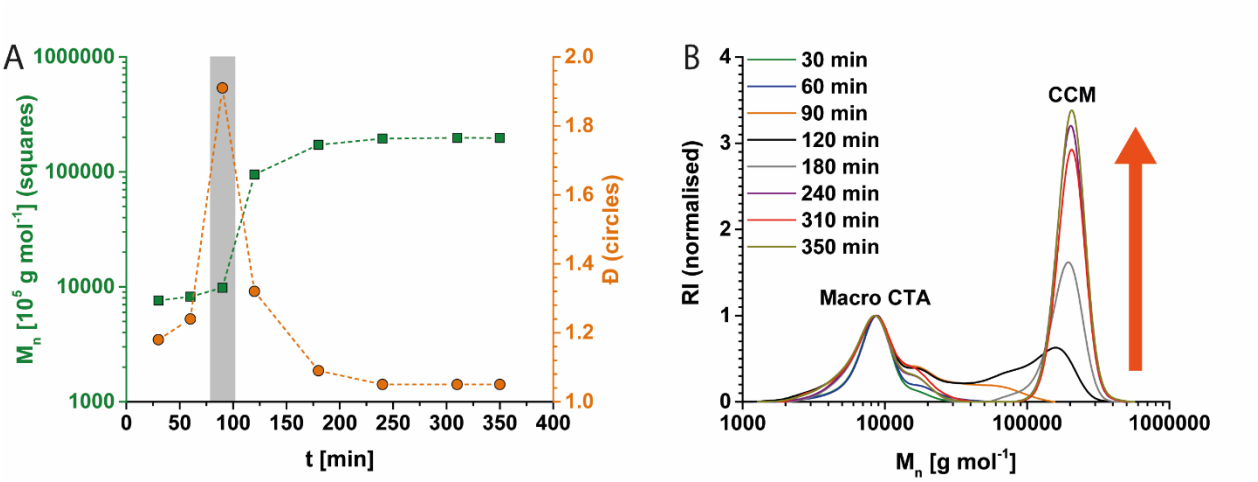

Figure 1. RAFT-mediated emulsion polymerisation followed by SEC (DMAc, PS-cal.) measurements. (A) Evolution of the molar mass and the dispersity. Grey box indicates the start of the polymerisation, as apparent from the spike in Đ due to the formation of a second distribution (see also (B) 90 min). From 120 min onwards (see also (B)), the M_n and Đ plotted refer to the CCMs. (B) Molar mass distribution at indicated time points. Red arrow indicates the increase of the CCMs relative to the macro CTA. Traces are normalised to the peak maximum of the macro CTA.

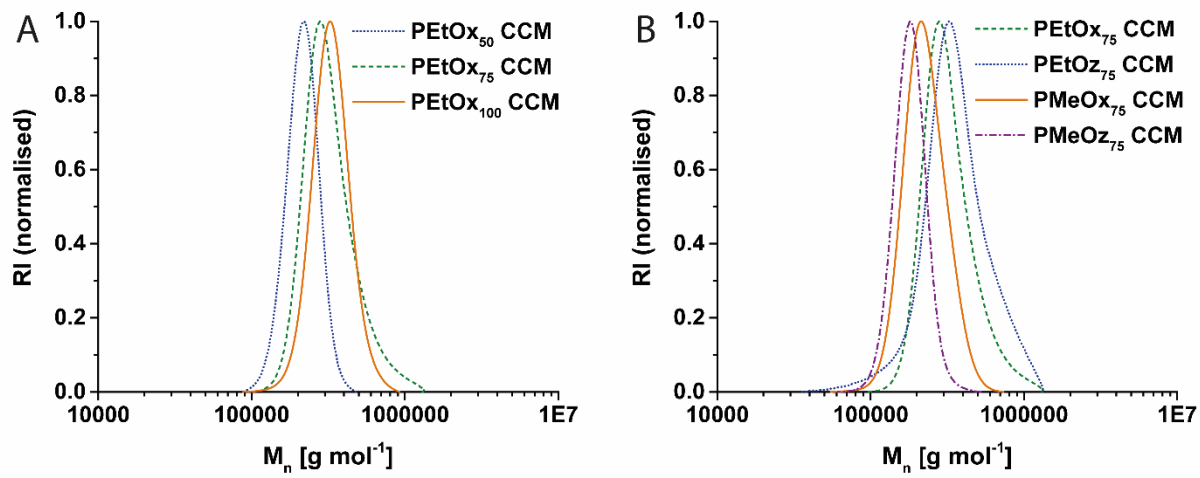

Figure 2. SEC (DMAc, PS-cal.) measurements of CCMs with (A) different $PEtOx_n$ shells, and (B) various PCIEs (DP = 75) shells.

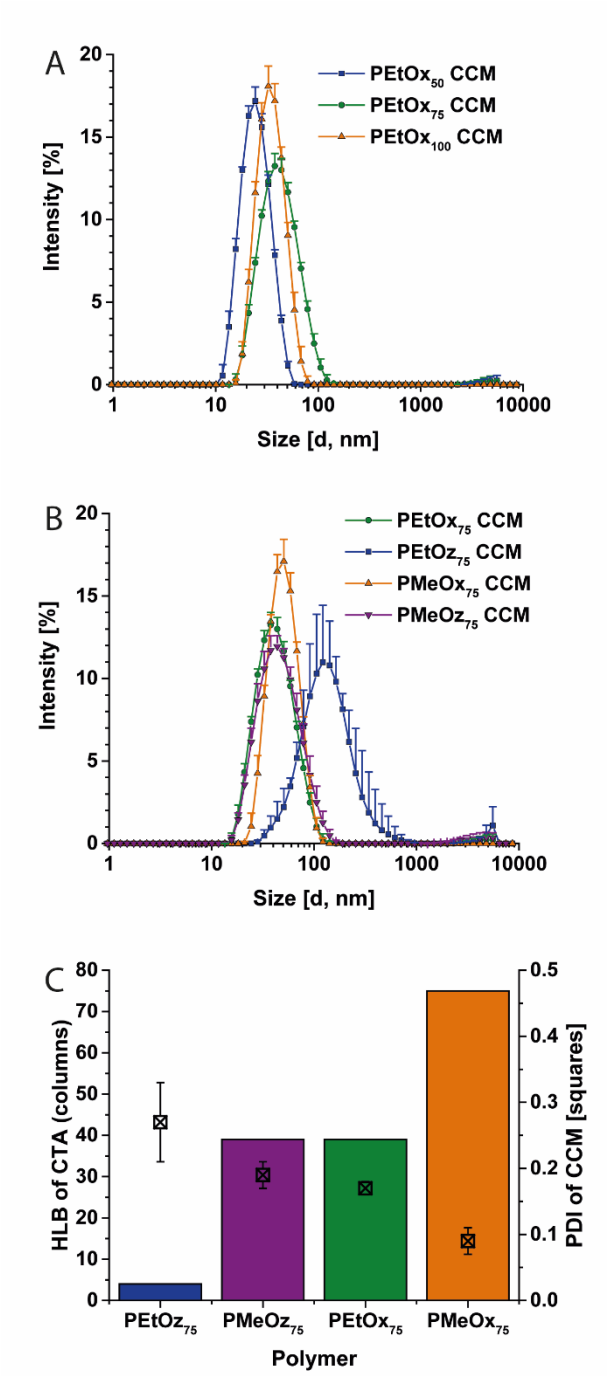

Figure 3. Characterisation of different CCMs. (A) and (B) Intensity size distributions (mean and SD) obtained by DLS measurements (1 mg mL^{-1}, PBS, 25 °C, average of 5 measurements with 3 runs each). (C) Dependence of CCM PDI determined by DLS measurements on HLB of macro CTA (average of 5 measurements with 3 runs each). HLB was calculated via the Davies method.[55]

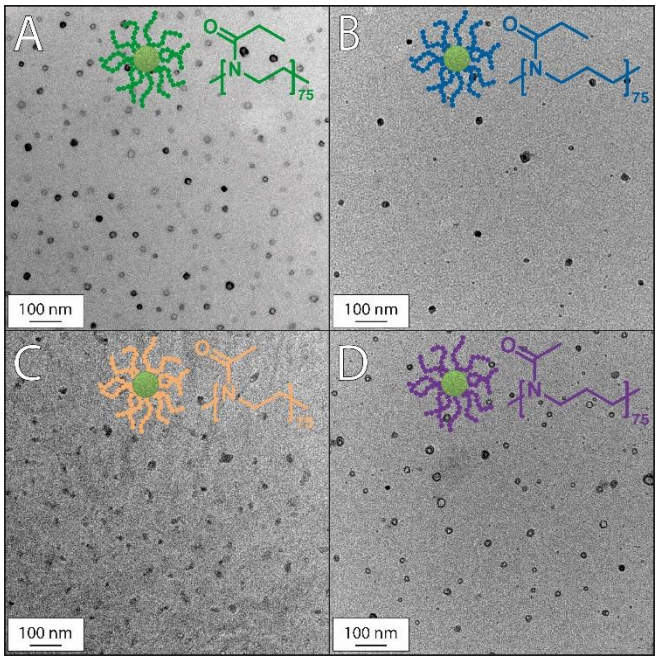

Figure 4. TEM images of CCMs with various PCIEs (DP = 75) shells. Samples were diluted in PBS at a concentration of 1 mg mL^{-1}, applied onto Formvar coated copper grids and washed to remove salt prior imaging. (A) $PEtOx_{75}$ CCM. (B) $PEtOz_{75}$ CCM. (C) $PMeOx_{75}$ CCM. (D) $PMeOz_{75}$ CCM.

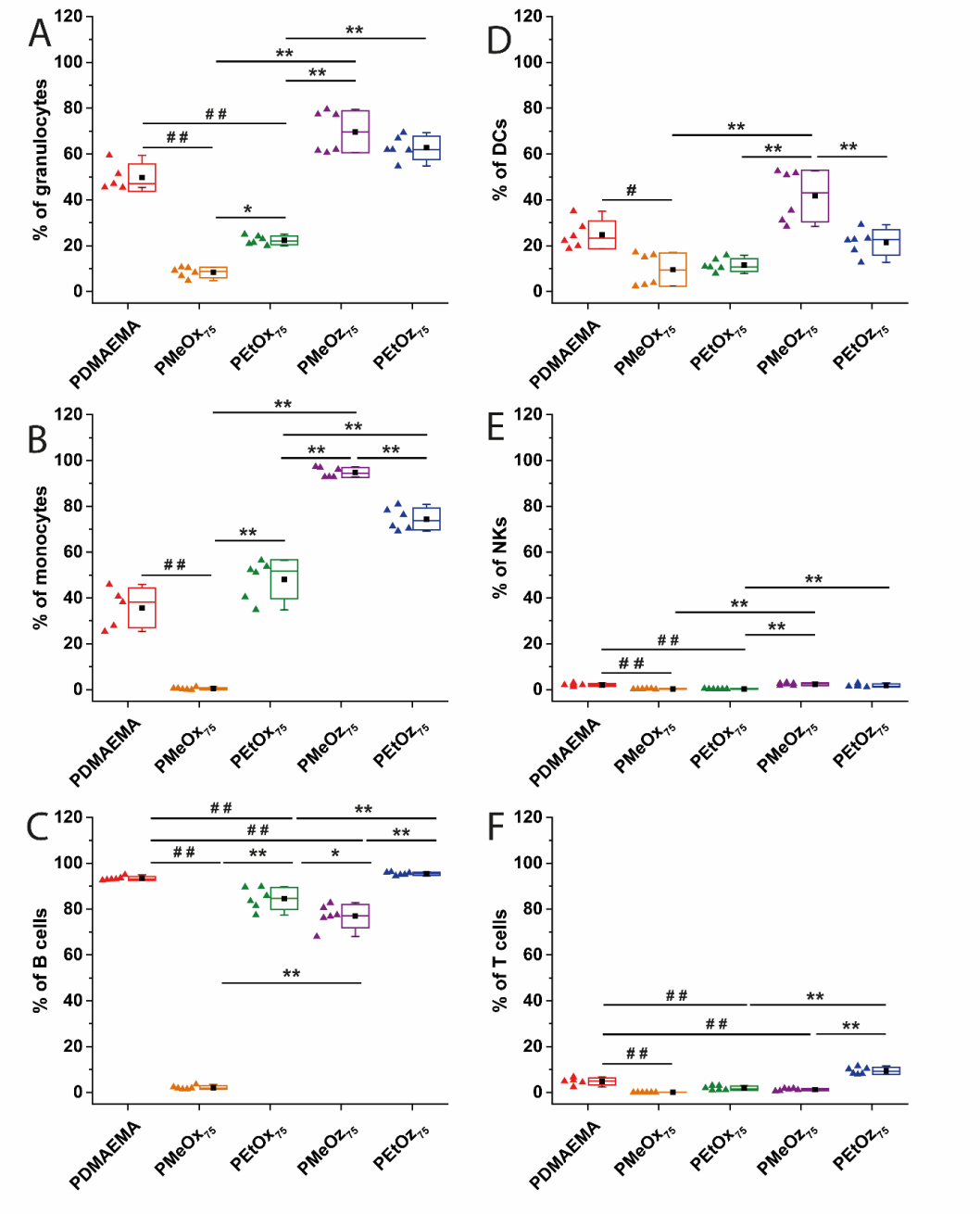

Figure 5. Association of PCIE CCMs with primary immune cells from whole blood. 10 µL Cy5 labelled CCMs (100 µg mL^{-1} in PBS) were incubated with 100 µL human blood at 37 °C for 1 h. Cellular association was determined by flow cytometry. Plots show the percentage of Cy5 positive cells of each population. Experiments were conducted in triplicates on two different days. Statistical analysis was conducted using a one-way ANOVA with Tukey test. */# $p < 0.005$. **/## $p < 0.0005$. # represents significant reduction of cellular association of PCIE CCMs compared to PDMAEMA CCMs. * represents significant differences within the PCIE CCMs. Boxes represent mean and SD. Whiskers represent min and max. Scatters depict actual data points. Values can be found in Table S3.

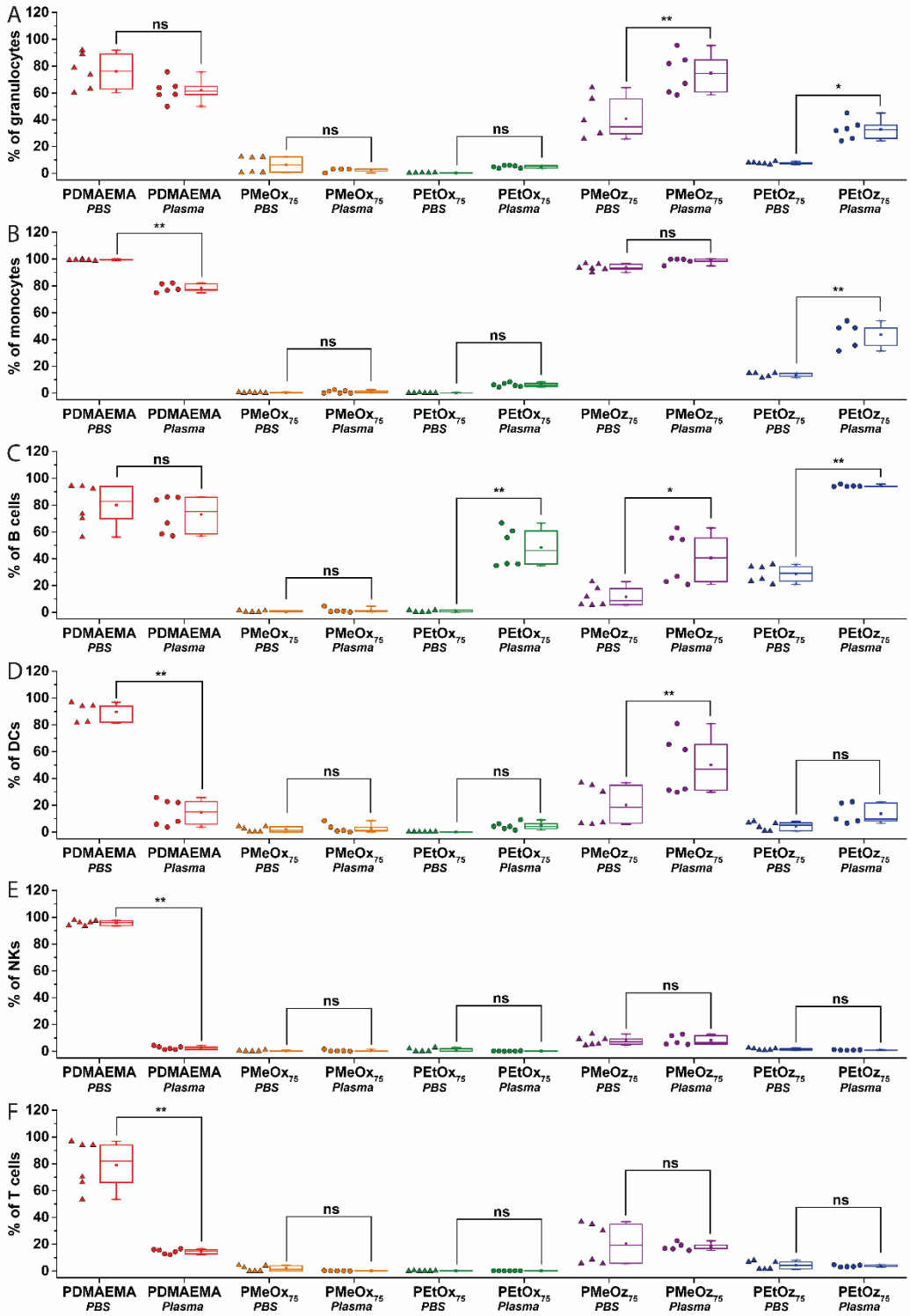

Figure 6. Association of PCIE CCMs with primary immune cells from washed blood. Cy5 labelled CCMs were pre-incubated in PBS or human plasms at a concentration of 100 µg mL^{-1} and, subsequently, 10 µL of CCM solution were added to 100 µL plasma free human blood and further incubated at 37 °C for 1 h. Cellular association was determined by flow cytometry. Plots show the percentage of Cy5 positive cells of each population. Experiments were conducted in triplicates on two different days. Statistical analysis was

conducted using a one-way ANOVA with Tukey test. * $p < 0.005$. ** $p < 0.0005$. ns not statistically significant. *Represents significant differences between samples with and without plasma incubation of the CCMs. Boxes represent mean and SD. Whiskers represent min and max. Scatters depict actual data points. Triangles: CCMs were incubated in PBS. Circles: CCMs were incubated in human plasma.

Table 1. Characterisation of CCMs.

CCMs	SEC[a]		DLS[b]			TEM[e]	
	M_n [g mol^{-1}]	Đ	d[c] [nm]	PDI[c]	T_{cp}[d] [°C]	d [nm]	PDI
PEtOx$_{50}$	207,900	1.06	37 ± 1	0.41 ± 0.00	66	18 ± 10	0.33
PEtOx$_{75}$	305,200	1.18	41 ± 1	0.19 ± 0.01	63	23 ± 7	0.11
PEtOx$_{100}$	317,000	1.09	34 ± 0	0.09 ± 0.01	64	15 ± 6	0.16
PEtOz$_{75}$	321,300	1.12	134 ± 3	0.21 ± 0.01	27	21 ± 7	0.12
PMeOx$_{75}$	215,000	1.11	49 ± 1	0.09 ± 0.02	None	21 ± 9	0.17
PMeOz$_{75}$	176,600	1.05	36 ± 1	0.18 ± 0.01	None	18 ± 6	0.11

[a]SEC in DMAc (PS-cal.). [b]DLS in phosphate buffered saline (PBS) (1 mg mL^{-1}), 5 measurements with 3 runs each. [c]25 °C. [d]Heating of the sample from 25 °C to 70°C. Temperature at which the CCMs show 50% size increase between onset and maximum of linear region. [e]Prepared from a 1 mg mL^{-1} solution in PBS.